Video Article

Visualization of High Speed Liquid Jet Impaction on a Moving Surface

Yuchen Guo[1], Sheldon Green[1]

[1]Department of Mechanical Engineering, University of British Columbia

Correspondence to: Sheldon Green at Sheldon.Green@ubc.ca

URL: https://www.jove.com/video/52603
DOI: doi:10.3791/52603

Keywords: Engineering, Issue 98, Liquid jet impingement, high-speed moving surface, spray nozzle, liquid friction modifier (LFM), air cannon, spinning disk, rail track lubrication, fluid mechanics

Date Published: 4/17/2015

Citation: Guo, Y., Green, S. Visualization of High Speed Liquid Jet Impaction on a Moving Surface. *J. Vis. Exp.* (98), e52603, doi:10.3791/52603 (2015).

Abstract

Two apparatuses for examining liquid jet impingement on a high-speed moving surface are described: an air cannon device (for examining surface speeds between 0 and 25 m/sec) and a spinning disk device (for examining surface speeds between 15 and 100 m/sec). The air cannon linear traverse is a pneumatic energy-powered system that is designed to accelerate a metal rail surface mounted on top of a wooden projectile. A pressurized cylinder fitted with a solenoid valve rapidly releases pressurized air into the barrel, forcing the projectile down the cannon barrel. The projectile travels beneath a spray nozzle, which impinges a liquid jet onto its metal upper surface, and the projectile then hits a stopping mechanism. A camera records the jet impingement, and a pressure transducer records the spray nozzle backpressure. The spinning disk set-up consists of a steel disk that reaches speeds of 500 to 3,000 rpm via a variable frequency drive (VFD) motor. A spray system similar to that of the air cannon generates a liquid jet that impinges onto the spinning disc, and cameras placed at several optical access points record the jet impingement. Video recordings of jet impingement processes are recorded and examined to determine whether the outcome of impingement is splash, splatter, or deposition. The apparatuses are the first that involve the high speed impingement of low-Reynolds-number liquid jets on high speed moving surfaces. In addition to its rail industry applications, the described technique may be used for technical and industrial purposes such as steelmaking and may be relevant to high-speed 3D printing.

Video Link

The video component of this article can be found at https://www.jove.com/video/52603/

Introduction

This research aims to determine strategies for applying LFM (Liquid Friction Modifier) in liquid jet form onto a moving surface while attaining high degrees of transfer efficiency and uniform deposition results. Achieving this objective involves developing a comprehensive understanding of factors that affect liquid jet impingement on moving surfaces.

The project is motivated by a need to improve the efficiency of lubrication application techniques used in the rail sector. As a means of reducing fuel consumption and locomotive maintenance costs, a thin film of friction modifying agent is now being applied to the upper rail surface of conventional railroad tracks. Recent studies have shown that applying one type of water-based LFM for top of rail (TOR) friction control reduced energy consumption levels by 6% and rail and wheel flange wear by in excess of 50%[1,2]. Other studies have shown that applying LFM to rail tracks reduces lateral force and noise levels as well as, more importantly, track corrugation and damage from rolling contact fatigue, which is a major cause of derailments[3,4]. These results were further confirmed in field tests on the Tokyo subway system[5].

LFMs are currently dispensed from air blast atomizers attached to dozens of locomotives throughout Canada and the United States. In this form of application, LFM is applied to the top of railroad tracks by atomizers mounted beneath moving rail cars. This mode of LFM application is difficult to implement on many railroad locomotives because the required high-volume and high-pressure air supply levels may not be attainable. Air-blast spray nozzles are also believed to produce highly irregular rail coverage when operated in a crosswind, as crosswinds cause fine spray droplets to deviate from their original trajectory. Crosswinds are also known to be implicated in nozzle fouling, likely for the same reason. Due to problems associated with air blast atomizers, the rail sector is currently seeking alternative approaches to LFM application onto rail tracks. One viable solution involves dispensing LFM by means of a continuous (not-atomized) liquid jet, as liquid jets are less susceptible to crosswind effects due to their lower drag-to-inertia ratio. Additionally, because the high air pressure and volume levels needed for atomizing nozzles are not required in liquid jet spray technologies, the latter act as more streamlined and robust spraying mechanisms that maintain effective control over the rate of LFM application.

An area of similar physics, droplet impingement, has been studied intensively. It was found by several researchers that for droplet impingement on a moving dry smooth surface, splashing behavior is dependent on many parameters including viscosity, density, surface tension and the normal component of the impact velocity[14,15]. Bird *et al.* demonstrated that both the normal and tangential velocities were of critical importance[16]. Range *et al.* and Crooks *et al.* have shown that for droplet impingement on a stationary dry surface, surface roughness decreases the splash threshold significantly (*i.e.*, it makes the droplet more prone to splash)[17,18].

Despite its practical importance, jet impingement on moving surfaces has received little attention in the academic literature. Chiu-Webster and Lister performed an extensive series of experiments that examined steady and unsteady viscous jet impingement on a moving surface, and the authors developed a model for the steady flow case[6]. Hlod *et al.* modeled the flow by means of a third-order ODE on a domain of unknown length under an additional integral condition and compared predicted configurations with experimental results[7]. However, the Reynolds numbers examined in both of these studies are much lower than those associated with typical railroad LFM applications. Gradeck *et al.* numerically and experimentally investigated the flow field of water jet impingement onto a moving substrate under various jet velocity, surface velocity, and nozzle diameter conditions[8]. Fujimoto *et al.* additionally investigated flow characteristics of a circular water jet impinging onto a moving substrate covered by a thin film of water[9]. However, these two projects used relatively large nozzle diameters and lower surface and jet velocities compared to those employed in the present work. Furthermore, though previous experimental, numerical, and analytical studies provide a large body of data, the majority have focused on heat transfer parameters rather than on liquid flow processes such as jet splashing behavior. The experimental method provided in the present research thus contributes to liquid jet application technologies by refining such techniques under conditions involving smaller jet nozzle diameters and high-speed jet and surface velocities. The present method also refines knowledge on fundamental fluid mechanics problems associated with moving contact lines.

The studies mentioned above have generally involved the interaction of a low speed jet with a low speed moving surface. There have been comparatively few studies of laminar high speed jet impingement onto high-speed moving surfaces. During high speed liquid jet impaction the jet liquid spreads radially in the vicinity of the impingement location, forming a thin lamella. This lamella is then convected downstream by the viscous forcing imposed by the moving surface, producing a characteristic U-shaped lamella. Keshavarz *et al.* have reported on experiments employing Newtonian and elastic liquid jets impinging onto high-speed surfaces. They classified impingement processes into two distinct types: “deposition” and “splash”[10]. For impingement to be classified as deposition, the jet liquid must adhere to the surface, whereas splash is characterized by a liquid lamella that separates from the surface, and subsequently breaks up into droplets. A third impingement regime has also been described — “splatter”. In this, comparatively rare, regime the lamella remains attached to the surface, as for “deposition”, but fine droplets are ejected from near the leading edge of the lamella. In a subsequent study of non-Newtonian fluid effects, Keshavarz *et al.* concluded that the splash/deposition threshold is mainly determined by the Reynolds and Deborah numbers, whereas the jet impingement angle and jet velocity to surface velocity ratios only have a minor effect[11]. In experiments conducted under variable ambient air pressures, Moulson *et al.* discovered that the splash/deposition threshold Reynolds number dramatically increases with decreasing ambient air pressure (*i.e.*, higher ambient pressures make jets more prone to splash), while decreasing ambient air pressure below a certain threshold suppresses splash completely[12]. This finding strongly suggests that aerodynamic forces acting on the lamella play a crucial role in causing lamella lift-off and subsequent splash. In recent work on high-speed impingement on a high-speed substrate, Sterling showed that for substrate speed and jet conditions close to the splash threshold, splash may be triggered by very small localized surface roughness and minor jet unsteadiness. He also showed that under these conditions lamella lift-off and reattachment is a stochastic process[13].

The experimental protocol described here may be used to study other physical situations involving the interaction of a fluid with a moving high speed surface. For example, the same approach could be used to study helicopter blade-vortex interaction (provided that the vortex fluid was colored with tracer particles) and robotic spraying of surfaces.

Protocol

1. Spinning Disk Device

1. Identify desired test conditions and record test conditions in a table (*e.g.,* ambient temperature, fluid properties, jet and surface speed, *etc.*).
2. Preparation of Materials
    1. Prepare glycerin-water or PEO-glycerin-water solutions for the impingement tests.
        1. In the case of PEO-glycerin-water tests, gradually dissolve 4.5 g of PEO powder (viscosity-average molecular weights of one million and four million) into 1495.5 g of distilled water under gentle magnetic stirring over a 24 hr period. Avoid excessively agitating the PEO sample to prevent mechanical degradation.
        2. Gradually add 1.5 kg of USP-grade glycerin to the aqueous PEO solution over a 24 hr period to reach an aqueous solution of 0.15% PEO concentration and 50% glycerine concentration.
    2. Store the test liquids separately in airtight containers under RT before and after each test to minimize evaporation, water absorption from ambient air and contamination. Characterize and spray liquids within five days of preparation.
3. Performance of Experiments
    1. Make sure the spinning disk air bearing's air supply valve is open and the pressure gauge reading is in the correct working range (60-80 psig). Clear anything that might impede the disk movement and turn the disk by hand in both directions 5 rotations to check for any problems with the disk and bearings.
    2. Clean and secure the compressed gas closed accumulator for test fluid pressurization. Pour 3 kg of test liquid into the fluid port of the 1-gallon accumulator.
    3. Connect the gas port of the accumulator to the nitrogen tank via a pressure regulator. Connect the fluid port of the accumulator to the jet spray nozzle.
4. Set up control system and high-speed imaging system.
    1. Start the spinning disk control software and VFD control software. Position two high-speed cine cameras 35 cm away from the impingement point and adjust the high magnification lenses to capture the impingement point from two angles.
    2. Adjust the 150 W fiber-optic light source to achieve an evenly lit background for best image quality (**Figure 1**). Power on the control system at this point to facilitate camera adjustment.
    3. Perform the self-check routine by clicking ‘Self-check’ button in the control software to make sure the system is functioning as expected.

5. Perform a jet impingement test
    1. Set the disk speed to the desired value with the VFD control software (500-3,000 rpm).
    2. To perform a test, launch the automated experimental sequence from the control software by clicking the 'Test sequence' button. The software will determine the optimal parameters automatically and coordinate each component of the system to perform the test accordingly.
    3. Save the resultant impingement test video (see, for example, the screen shot in **Figure 2**). Read and record surface speed, nozzle back pressure and temperature from the control software.
    Note: After each test, a disk cleaning sequence runs automatically to rinse and dry the disk surface. Repeat the cleaning cycle as necessary until all test fluid residue has been removed.
    CAUTION: While water and glycerin solution test fluids may be cleaned with the cleaning sequence, other LFMs need to be cleaned with organic solvents such as acetone. In such cases, apply the cleaning material to a cloth rather than spraying the disk directly.

6. Data Analysis
    1. Prepare a spreadsheet containing information on each test condition (*e.g.*, fluid properties, ambient temperature, surface roughness, *etc.*).
    2. Open the recorded jet impingement images with cine viewing software, play full video recordings at normal speed and observe jet impingement behaviors.
    3. Record impingement behavior characteristics (splash/spattering/deposition; see **Figure 3**) in the prepared spreadsheet, logging any unusual trends that may indicate complications with the experimental set-up.
    4. Save test results and conditions in a spreadsheet. Record notable findings and unusual occurrences in test log (*e.g.,* splash/deposition threshold point, splash/deposition transitions, *etc.*). Save screenshots when necessary.
    5. Conduct image analysis measurements and record data.
        1. Launch the on-screen pixel measuring tool. Open impingement images, and calibrate the image scale by measuring a micro-ruler in the images with the on-screen pixel measuring tool (**Figure 4**).
        2. Measure dimensions of interest (*e.g.*, lamella spread width, W, and lamella stagnation point radius, R; see **Figure 5**) with the pixel measuring tool at a point where the jet appears to be most stable in the video and record data in the prepared spreadsheet. Then take another group of measurements 100 frames after the first group of measurements to confirm that both the jet and the lamella are stable. Plot data points on a graph and complete the curve fitting.

2. Air Cannon Device

1. Identify desired test conditions and prepare materials as in step 1.1 and step 1.2.
2. Performance of Experiments
    1. Power up the system-control software.
    2. Insert the projectile into the cannon barrel. Move the stop mechanism close to the barrel exit to properly capture the projectile after a test (**Figure 6**).
    3. Open the pressurized building air line leading to the air tank. Pressurize the tank to between 30 psi and 70 psi, depending on the desired projectile velocity. 30 psi tank pressure gives a projectile speed of around 5 m/sec, and 70 psi gives a speed of around 25 m/sec.
    4. Prepare the compressed gas closed accumulator for test fluid pressurization.
        1. Pour 3 kg of test liquid into the fluid port of the accumulator. Connect tubing from the accumulator gas valve to the liquid jet spray nozzle, and set the accumulator pressure to up to 300 psig.
    5. Attach the camera to the scissor jack. Secure the scissor jack to the platform positioned next to the jet spray nozzle.
    6. Secure the high-intensity light source to the platform positioned across from the camera and behind the diffusion sheet. Check lighting and camera positioning using the video camera viewing function of the software control interface, and adjust positioning as necessary (**Figure 7**).
    7. Put on earmuffs for protection from the air cannon sound blast.
    8. Unlock the cannon control panel, and press the warning button on the control panel multiple times to signal the start of an experiment.
    9. Hit the control panel button that opens the solenoid valve connecting the air tank with the air cannon barrel.
    10. After the device has been fired and the projectile captured, clean the device by wiping it with cleaning fluid and a sponge to remove residual test fluid. Finally, dry the impingement surface of the projectile.

3. Measure speed of the projectile in the recorded high-speed video by measuring the amount of time required for the projectile to travel a fixed (10 cm) distance. Analyze data as in step 1.5.

Representative Results

As discussed in the introductory section, the three main behaviors associated with liquid jet impingement are deposition, splatter and splash. These jet impingement behaviors are observed using video data recorded by high-speed cine cameras positioned at various optical points. Examples of still images, obtained from the video recordings, which depict the three liquid jet outcomes are shown in **Figure 3**. **Figure 3A** depicts liquid jet deposition, in which the jet flows in a completely straight and steady stream towards the impingement surface. The jet adheres to the surface and remains on the surface for the remainder of the experiment. **Figures 3B** and **3C** show less optimal results in which the liquid jet only partially adheres to the impingement surface, with the remainder of the jet either splattering (**Figure 3B**) or splashing (**Figure 3C**) upon impact.

Given the fairly straightforward nature of the given video data, ambiguous results are uncommon and repeatable results have been obtained from both experimental devices. However, in very rare cases that typically involve very smooth surface roughness conditions, the lamella of a liquid jet stream may interact with droplets or roughness on the surface in such a way that causes it to lift off from the impingement surface (**Figure 8**). In equally unusual circumstances, a small disturbance in the flow can produce irregularities in the jet, which upon surface impaction become amplified, causing the jet to separate from the surface for a long period of time (**Figure 9**). These rare phenomena typically occur only for high surface speeds and for intermediate jet fluid viscosities (Re = 100~2,500). The consistency of results is largely credited to the use of a pressure accumulator for driving the test liquid, which, unlike a pump, propels liquid at a constant rate, producing a very smooth action and thus a highly consistent, uniform and steady liquid flow.

With respect to splash/deposition characteristics, the results show that for metal surfaces of average roughness heights ranging between 0.01 µm and 1 µm, decreasing the surface roughness makes the impinging jet more susceptible to splash. For example, **Figure 3A** and **Figure 3C** show impingement under similar jet and surface speed conditions. In **Figure 3A** jet deposition occurs on the surface, which has an average roughness height of 0.51 µm, but jet splash occurs when the average roughness height is 0.016 µm (**Figure 3C**). This dependence on roughness is opposite to that observed by Keshavarz *et al.*[10,11], who studied impingement on much rougher surfaces, where the surface roughness is significantly larger than the lamella thickness.

The threshold of splash is a complex function of the liquid jet velocity; liquid jet diameter; liquid viscosity, density and surface tension; the surface speed and roughness; and the surrounding air characteristics. Although some simple theories of splash have been proposed[10-12], there is currently no comprehensive explanation of the phenomenon. Lamella liftoff, which is usually a precursor to splash[12], is believed to be a function of lamella geometry. As seen in **Figure 10**, the lamella geometry is itself a complex function of many variables, including the jet and surface speeds and liquid physical properties.

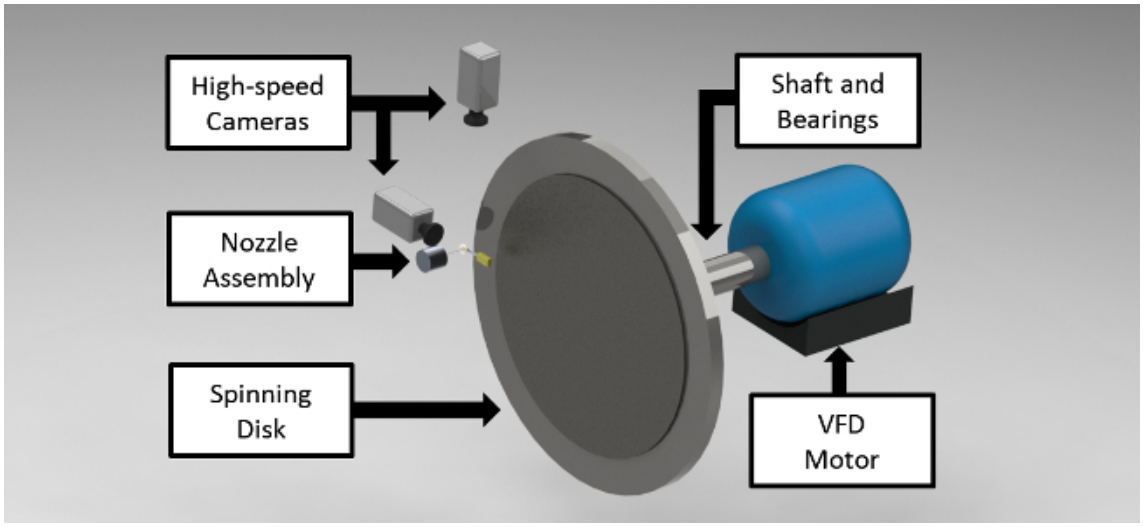

Figure 1. Schematic of optical configuration of spinning disk device. Please click here to view a larger version of this figure.

Figure 2. Screenshot of typical video recording. Please click here to view a larger version of this figure.

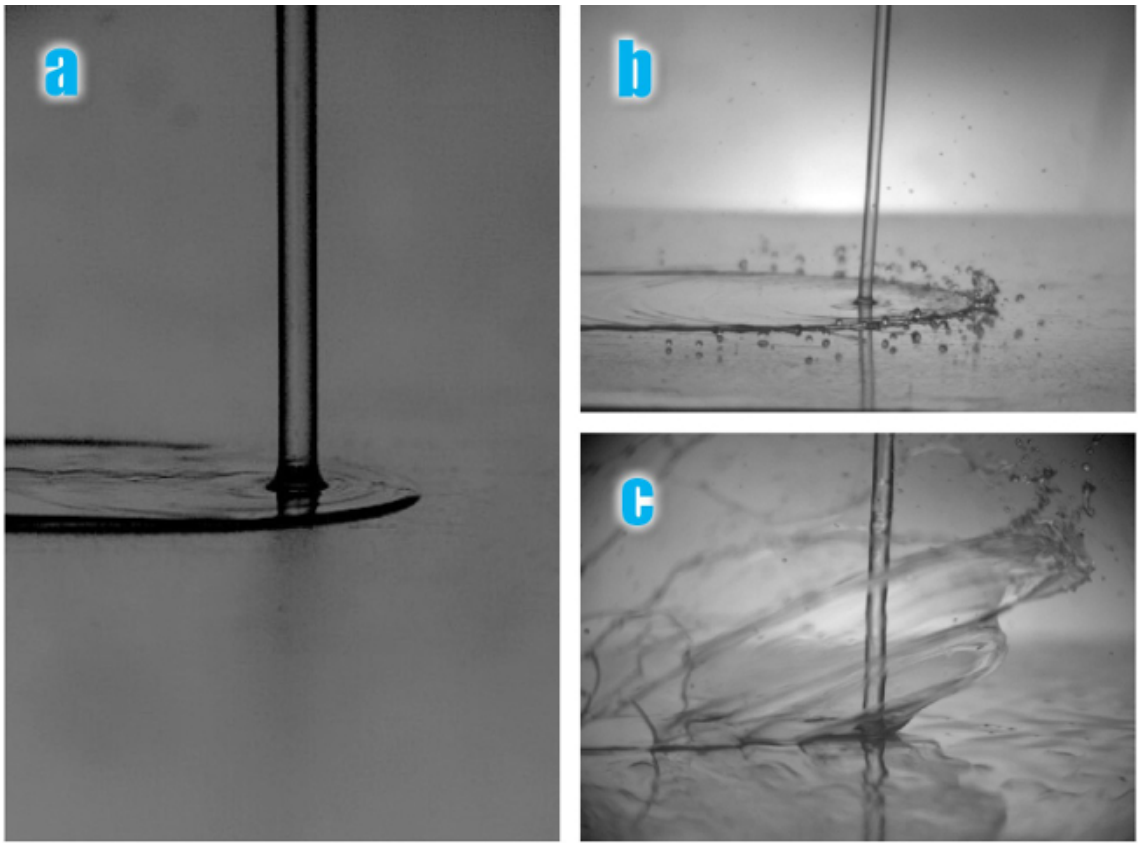

Figure 3. Three typical flow regimes. (**A**) deposition, (**B**) splatter, (**C**) splash. In all instances the substrate moves from right to left and the jet diameter is 564 µm. The relevant jet and substrate conditions are: (**A**) V_{jet} = 18.3 m/sec, $V_{substrate}$ = 7.50 m/sec, μ_{jet} = 0.0194 N·sec/m^2, ρ_{jet} = 1,180 kg/m^3, σ_{jet} = 0.0656 N/m, Re_{jet} = 629, We_{jet} = 3,400; (**B**) V_{jet} = 9.5 m/sec, $V_{substrate}$ = 7.63 m/sec, μ_{jet} = 0.0097 N·sec/m^2, ρ_{jet} = 998 kg/m^3, σ_{jet} = 0.0717 N/m, Re_{jet} = 552, We_{jet} = 709; (**C**) V_{jet} = 17.3 m/sec, $V_{substrate}$ = 7.71 m/sec, μ_{jet} = 0.0194 N·sec/m^2, ρ_{jet} = 1,180 kg/m^3, σ_{jet} = 0.0656 N/m, Re_{jet} = 594, We_{jet} = 3,040. Please click here to view a larger version of this figure.

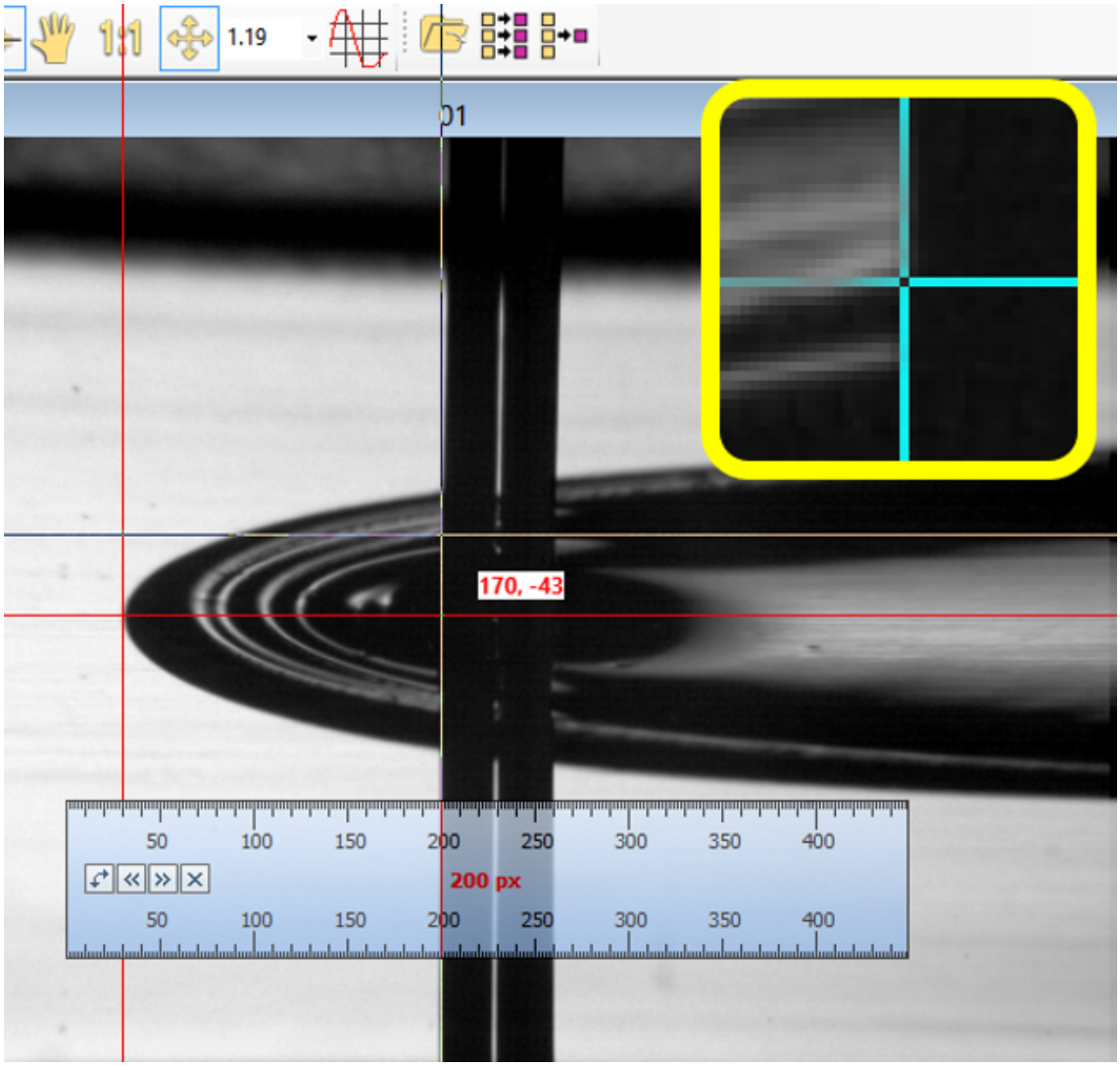

Figure 4. Measurement of jet diameter and lamella geometry with image processing software. Please click here to view a larger version of this figure.

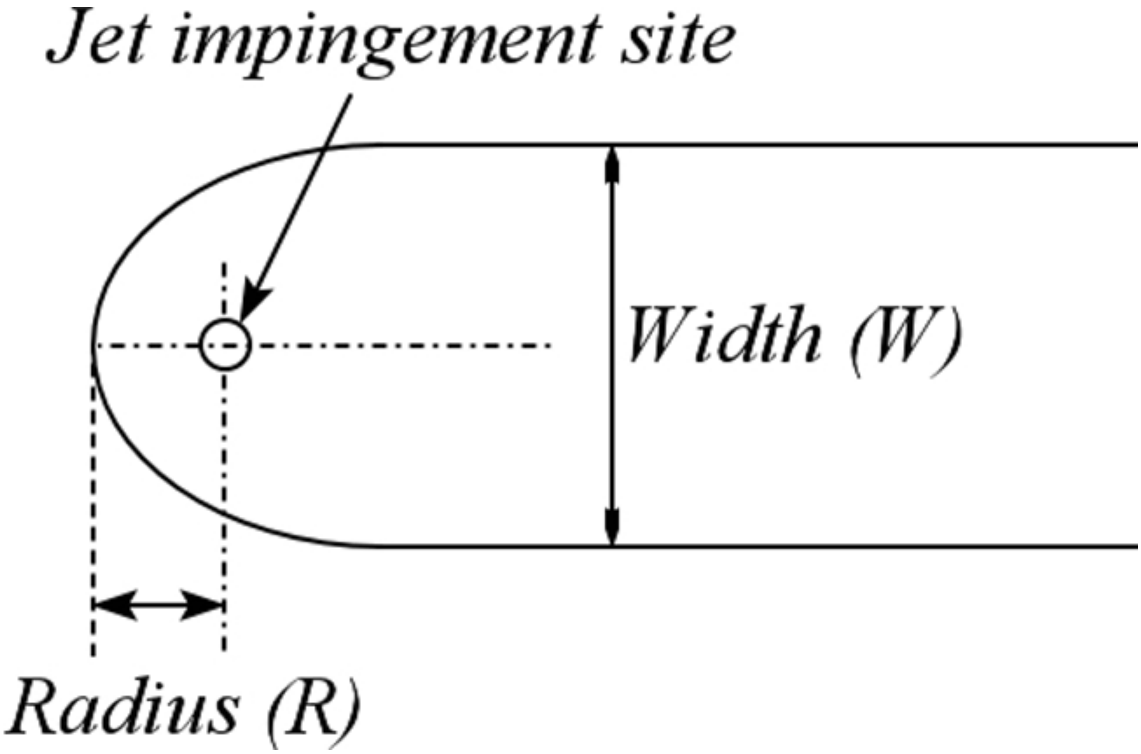

Figure 5. Planform view schematic of jet impingement showing characteristic lamella dimensions. Please click here to view a larger version of this figure.

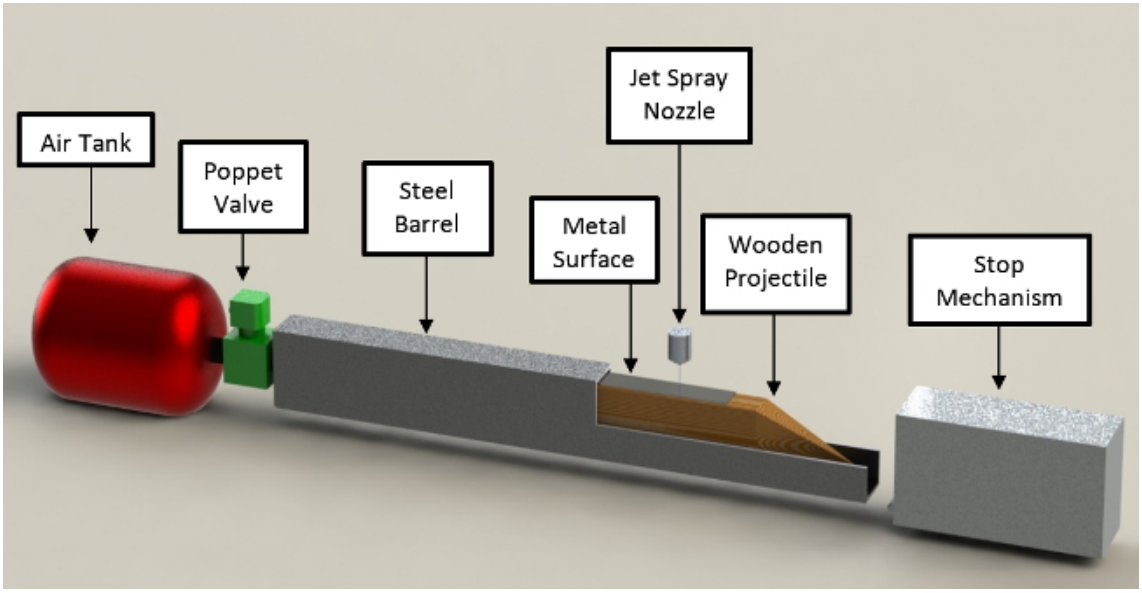

Figure 6. Air cannon mechanical configuration. Please click here to view a larger version of this figure.

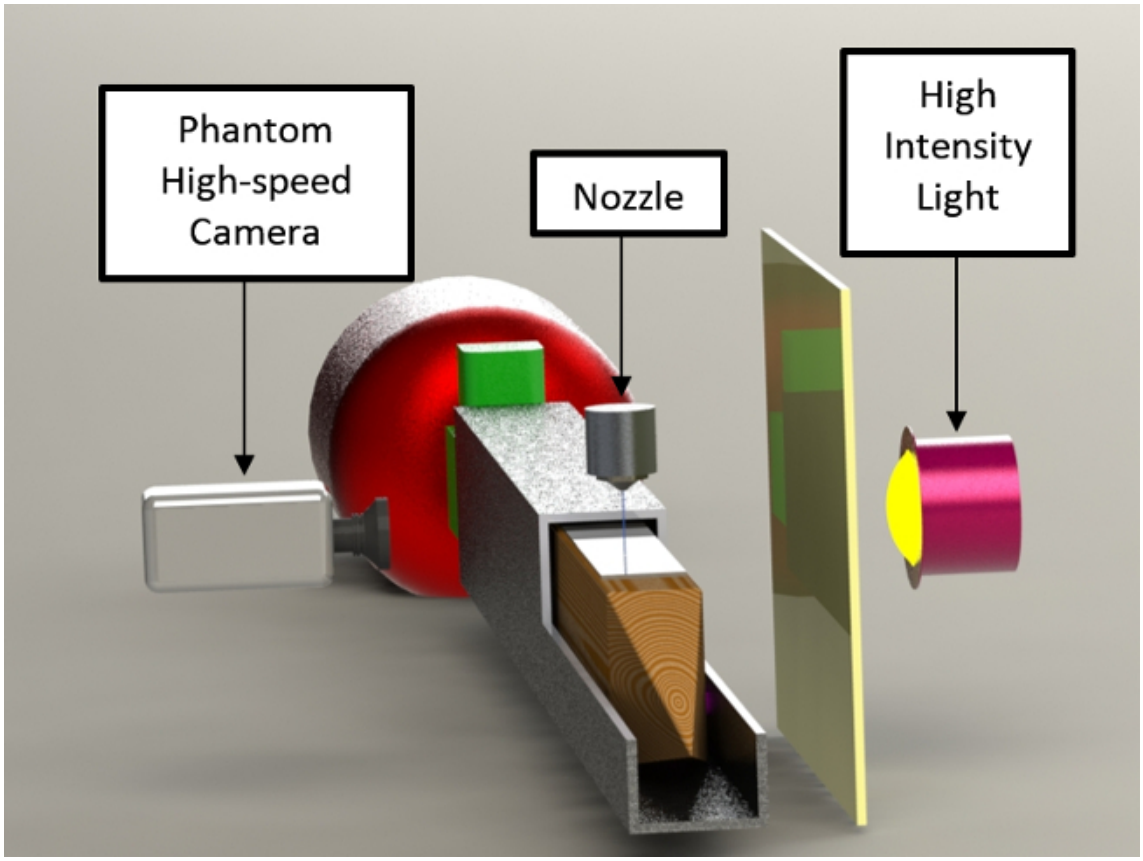

Figure 7. Air cannon optical configuration. Please click here to view a larger version of this figure.

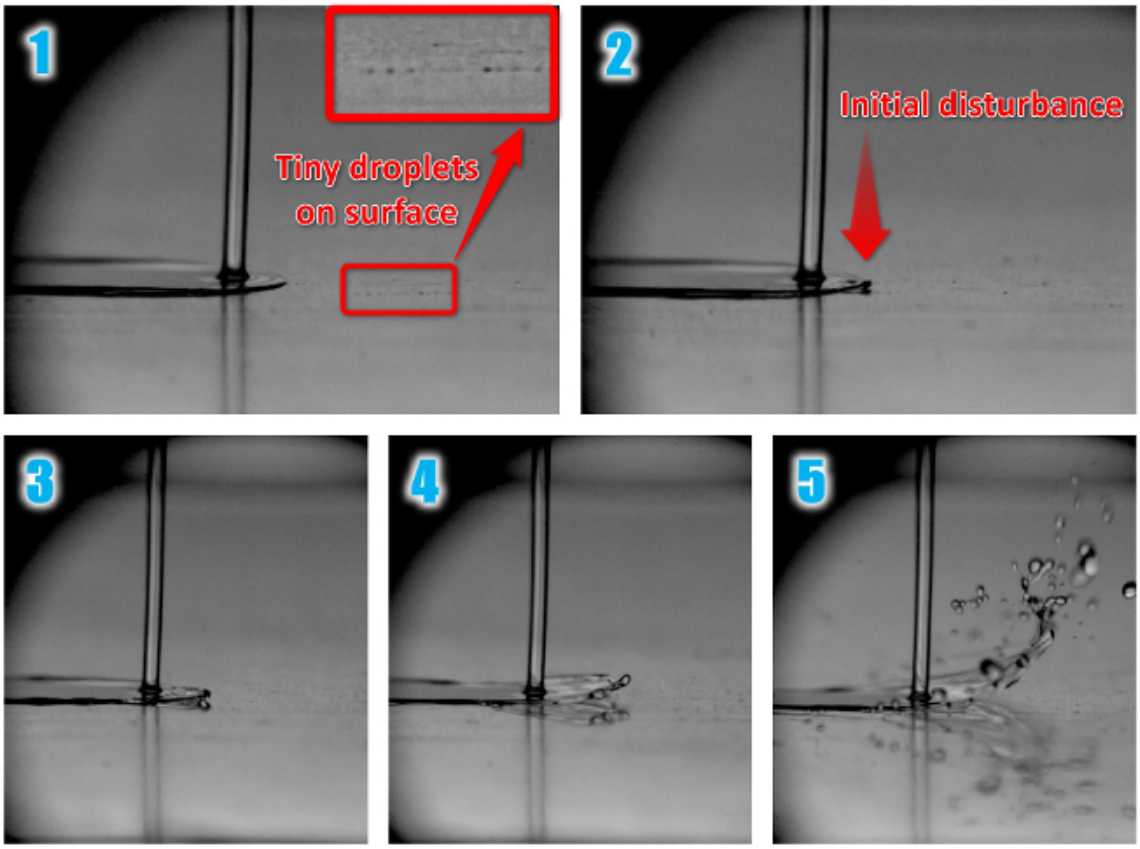

Figure 8. Time sequence showing the transition from jet deposition to jet splash. In this sequence the transition is caused by very fine droplets adhering to the otherwise dry substrate. The substrate is moving from right to left at a speed $V_{substrate}$ = 7.52 m/sec. The jet conditions are: D_{jet} = 564 µm; V_{jet} = 17.5 m/sec, μ_{jet} = 0.0194 N·sec/m^2, ρ_{jet} = 1,180 kg/m^3, σ_{jet} = 0.0656 N/m, Re_{jet} = 600, We_{jet} = 3,110. Please click here to view a larger version of this figure.

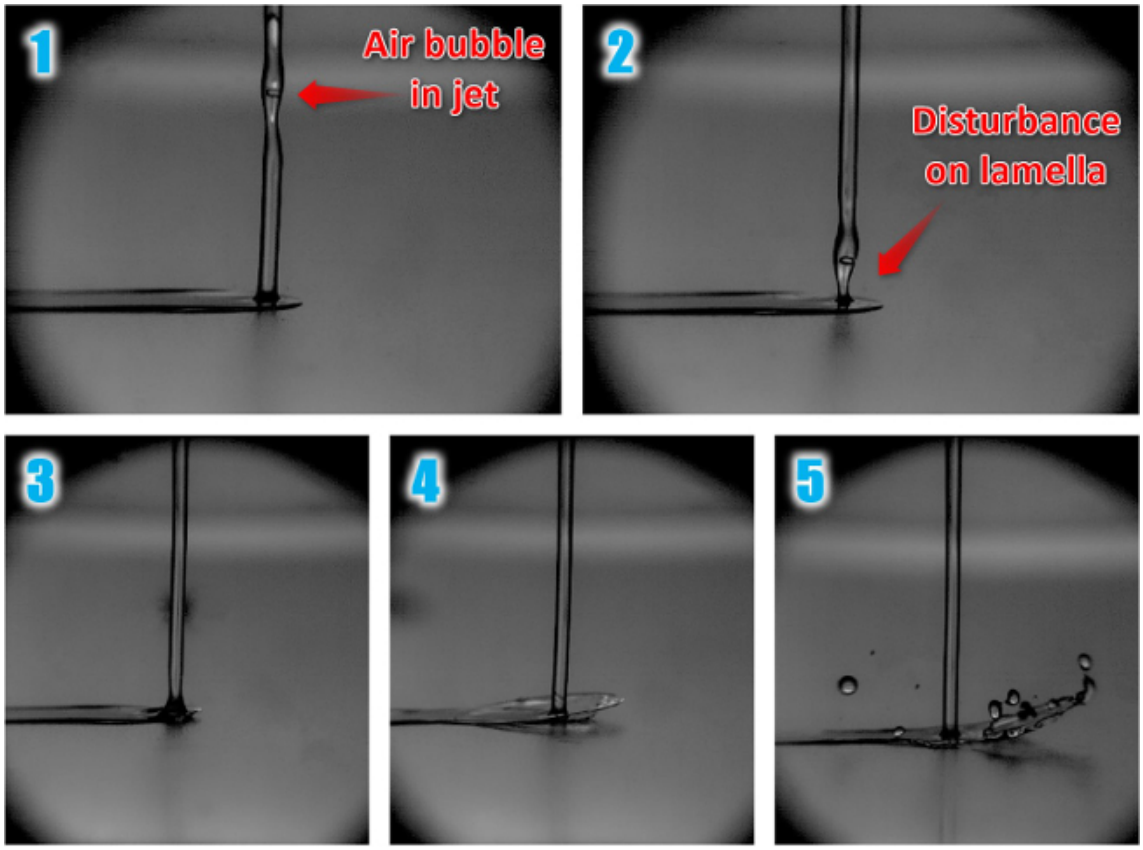

Figure 9. Time sequence showing the transition from jet deposition to jet splash. In this sequence the transition is caused by a small air bubble in the jet that perturbs the flow. The substrate is moving from right to left at a speed $V_{substrate}$ = 7.43 m/sec. The jet conditions are: D_{jet} = 564 µm; V_{jet} = 15.8 m/sec, μ_{jet} = 0.0194 N·sec/m^2, ρ_{jet} = 1,180 kg/m^3, σ_{jet} = 0.0656 N/m, Re_{jet} = 542, We_{jet} = 2,530. Please click here to view a larger version of this figure.

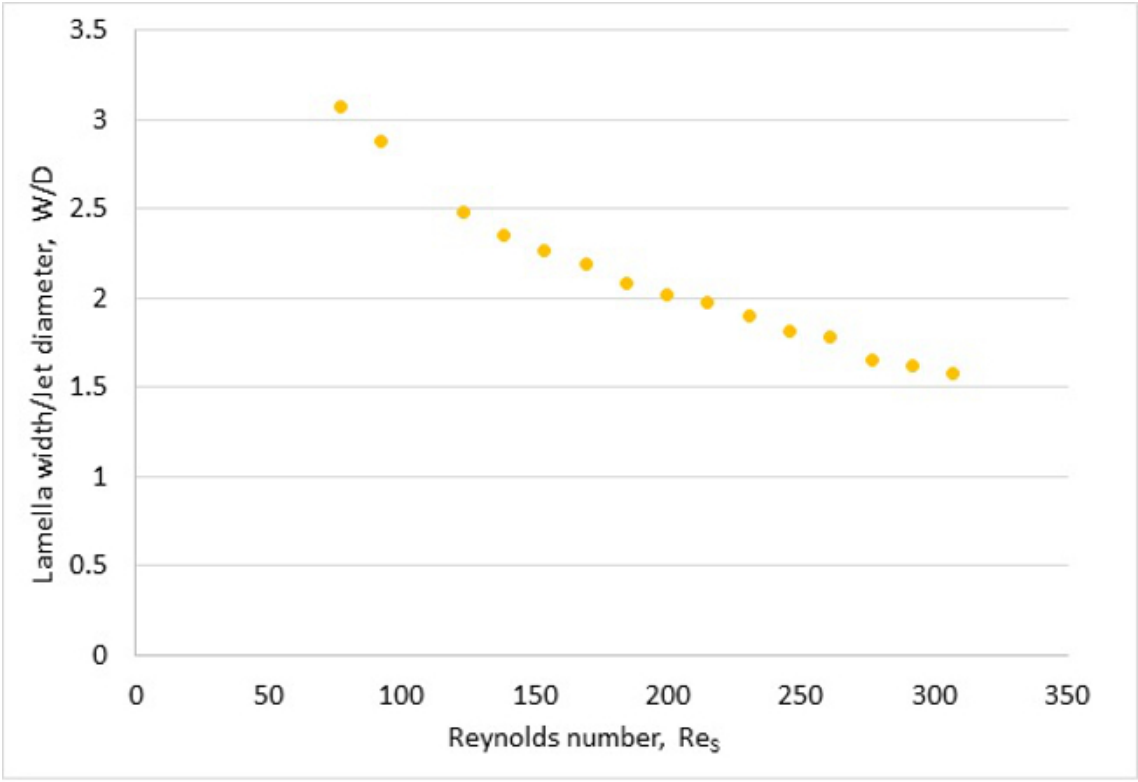

Figure 10. Lamella spread width to jet diameter ratio, as a function of Reynolds number of substrate. Substrate speed $V_{substrate}$ is varied from 15 m/sec to 60 m/sec, giving a Reynolds number Re_S of 75 to 300. The jet conditions are: D_{jet} = 281 µm; V_{jet} =14.6 m/sec, μ_{jet} = 0.0701 N·sec/m^2, ρ_{jet} = 1,220 kg/m^3, σ_{jet} = 0.0640 N/m, Re_{jet} = 71.4, We_{jet} = 1,140.

Discussion

The projectile used for the air cannon set-up is composed of a lightweight, wooden base. Though the wooden material chips slightly after numerous tests, it has been found to absorb kinetic energy more effectively than projectiles composed of materials such as plastic or metal, which tend to shatter upon impacting the stop mechanism. The dimensions of the wooden projectile are designed to closely match the steel barrel interior, thus restricting air leakage. A 1/8" thick rubber sheet secured between two layers of plywood is attached to the back of the projectile to further tighten the seal around the inside of the barrel. The metal impingement surfaces mounted on top of the projectile are fastened as three separate metal plates of different roughness heights, positioned 2.5 cm apart, so that the liquid jet can impinge on all three surfaces in one test with minimal interference. The front of the projectile is shaped into an aerodynamic nose with a barb on the bottom of the nose so that the stop mechanism, which has a heavy aluminum body with a latch mechanism inside, connects securely to the projectile upon impact. Rather than being fixed in place, the stop mechanism slides backwards by roughly 60 cm upon catching the projectile. This function dissipates kinetic energy from the projectile and prevents material damage.

The high-speed cine camera attached to the air cannon device visualizes jet impaction on the projectile surface. The camera's wide-screen CMOS sensor allows one to capture images at extremely high frame rates and resolutions. A 1 kW, high-intensity incandescent light source is used to illuminate the field of view, and a light diffusor sheet is placed between the light source and the impingement point to achieve an evenly lit background. Two cameras and light sources are installed on the spinning disk device to capture video recordings from more than one angle. One camera positioned above the impingement point records the front view of the jet impingement, while the second camera records a side view. The camera lenses are covered with a sheet of acetate film to prevent contact with test fluids and to provide a clear viewing window after each test. The side-view camera is illuminated by a high-intensity, fiber-optic light source that locally illuminates the impingement site without blocking the axle. The front-view camera is illuminated by a high-intensity, 100 W, 6,700 Lumen white LED array fitted with a collimating lens.

The two experimental set-ups are controlled electrically by two custom-built control boxes. The custom-built control software allows the user to generate and collect digital and analog signals through a USB DAQ system inside the control box. A controller then utilizes these signals to control each component of the experimental set-up (high-speed camera, light, nozzle, *etc.*).

The described experimental set-up is limited in that two separate machines were built to test a broad range of surface speeds. The air cannon device can only be operated at slower speeds because it is very difficult to stop non-destructively a projectile moving at velocities higher than 25 m/sec, within the limited space of a laboratory. With the spinning disk there was concern that the rotary motion of the disk would cause associated centripetal forces on the fluid, which would in turn affect the fluid mechanics. This concern proved to be unwarranted as testing with the same jet conditions and same surface speeds on the air cannon (linear surface velocity) and the spinning disk yielded almost identical impaction characteristics. The maximum allowed Reynolds number is limited by liquid jet breakup. In the experiments conducted on these set-ups, a Reynolds number of 1,500 was easily reached. Substrate speed on the high-speed set-up is limited by the capacity of the VFD motor (*i.e.,* maximum rotational speed and maximum power output to overcome drag, inertia, *etc.*), provided the disk and shaft are well balanced.

The described apparatuses differ from existing techniques that examine liquid jet impingement in that they accommodate the study of high-speed liquid jet impingement over high surface speed conditions (25-100 m/sec) using small liquid jet nozzle diameters. Because liquid jet impingement processes that occur on stationary and low-speed moving surfaces differ considerably from those associated with high-speed moving surfaces with respect to liquid build-up and spread patterns, the described technique can further existing knowledge on liquid jet impingement behaviors under a broader range of conditions. The technique's focus on splash, splatter and deposition processes associated with liquid jet impingement also addresses a knowledge gap in this field, which has previously been preoccupied with heat transfer patterns. As liquid jet impingement onto a substrate is a highly complex multiphase fluid mechanics problem that poses many possible avenues for future research, the described technique may be used for a number of technical and industrial applications such as steelmaking and ink-jet printing, cooling, heating and surface coating.

Disclosures

The authors have nothing to disclose.

Acknowledgements

The Natural Sciences and Engineering Research Council of Canada (NSERC) and L.B. Foster Rail Technologies, Corp. jointly supported this research through the NSERC Collaborative Research and Development Grant program.

References

1. Cotter, J., *et al.* Top of Rail Friction Control: Reductions in Fuel and Greenhouse Gas Emissions. *Proc. Of the 2005 Conference of the International Heavy Haul Association (Rio de Janeiro).* 327-334 (2005).
2. Eadie, D. T., Bovey, E., Kalousek, J. The role of friction control in effective management of the wheel/rail interface). *Railway Technical Conference.* (2002).
3. Stock, R., Eadie, D. T., Elvidge, D., Oldknow, K. Influencing rolling contact fatigue through top of rail friction modifier application–A full scale wheel–rail test rig study. *Wear.* **271**, (1), 134-142 (2011).
4. Eadie, D. T., Santoro, M. Top-of-rail friction control for curve noise mitigation and corrugation rate reduction. *Journal of Sound and Vibration.* **293**, (3), 747-757 (2006).
5. Tomeoka, M., Kabe, N., Tanimoto, M., Miyauchi, E., Nakata, M. Friction control between wheel and rail by means of on-board lubrication. *Wear.* **253**, (1), 124-129 (2002).
6. Chiu-Webster, S., Lister, J. R. The fall of a viscous thread onto a moving surface: a 'fluid-mechanical sewing machine. *Journal of Fluid Mechanics.* **569**, (1), 124-129 (2006).
7. Hlod, A., Aarts, A. C. T., Van De Ven, A. A. F., Peletier, M. A. Mathematical model of falling of a viscous jet onto a moving surface. *European Journal of Applied Mathematics.* **18**, (06), 659-677 (2007).
8. Gradeck, M., Kouachi, A., Dani, A., Arnoult, D., Borean, J. L. Experimental and numerical study of the hydraulic jump of an impinging jet on a moving surface. *Experimental Thermal and Fluid Science.* **30**, (3), 193-201 (2006).
9. Fujimoto, H., Suzuki, Y., Hama, T., Takuda, H. Flow Characteristics of Circular Liquid Jet Impinging on a Moving Surface Covered with a Water Film. *ISIJ international.* **51**, (9), 1497-1505 (2011).
10. Keshavarz, B., Green, S. I., Davy, M. H., Eadie, D. T. Newtonian liquid jet impaction on a high-speed moving surface. *International Journal of Heat and Fluid Flow.* **32**, (6), 1216-1225 (2011).
11. Keshavarz, B., Green, S. I., Eadie, D. T. Elastic liquid jet impaction on a high speed moving surface. *AIChE Journal.* **58**, (11), 3568-3577 (2012).
12. Moulson, J. B. T., Green, S. I. Effect of ambient air on liquid jet impingement on a moving substrate. *Physics of Fluids.* **25**, (10), 102106 (2013).
13. Sterling, G. E. G. An experimental study on jet impingement on a very high speed moving surface. *UBC M.A.Sc. Thesis.* (2012).
14. Povarov, O. A., Nazarov, O. I., Ignat'evskaya, L. A., Nikol'skii, A. I. Interaction of drops with boundary layer on rotating surfaces. *Journal of Engineering Physics and Thermophysics.* **31**, (6), 1453-1456 (1976).
15. Fathi, S., Dickens, P., Fouchal, F. Regimes of droplet train impact on a moving surface in an additive manufacturing process. *Journal of Materials Processing Technology.* **210**, (3), 550-559 (2010).
16. Bird, J. C., Tsai, S. S., Stone, H. A. Inclined to splash: triggering and inhibiting a splash with tangential velocity. *New Journal of Physics.* **11**, (6), 063017 (2009).
17. Range, K., Feuillebois, F. Influence of surface roughness on liquid drop impact. *Journal of Colloid and Interface science.* **203**, (1), 16-30 (1998).
18. Crooks, R., Boger, D. V. Influence of fluid elasticity on drops impacting on dry surfaces. *Journal of Rheology.* **44**, (4), 973-996 (2000).

